

¹³C ENDOR Studies of Organic Doublet and Triplet State Molecules

B. Kirste, H. Kurreck,* W. Lubitz, and K. Schubert

Contribution from the Institut für Organische Chemie, Freie Universität Berlin, Thielallee 63-67, 1000 Berlin 33, Germany. Received August 16, 1977

Abstract: ESR, proton, and ¹³C ENDOR experiments have been performed on ¹³C labeled galvinoxyls in the doublet and triplet spin states. The measured hyperfine splitting constants were assigned to molecular positions. The relative signs of proton and carbon-13 couplings could be determined by using the novel electron nuclear nuclear TRIPLE resonance technique. The influence of temperature-dependent dynamic processes within the galvinoxyl systems on the magnitude of the ¹³C hyperfine constant was measured. From the ESR glass spectrum of the biradical the zero-field splitting parameters, the anisotropic g values, and all principal values of the HFS tensor of the ¹³C nucleus could be extracted. The ENDOR conditions to achieve optimum ¹³C signals for the monoradicals and the biradical studied are discussed and compared to those for the protons. It is shown that the difference in ENDOR conditions for the ¹³C nucleus and the galvinoxyl ring protons can be explained entirely by the magnitude of the HFS anisotropies of these nuclei. In the biradical *M_s* = 0 spin state both the "free nucleus lines" of protons and ¹³C could be observed by ENDOR in glassy solution. The synthesis of the ¹³C labeled galvinoxyl precursors, i.e., the galvinoxyls, is given.

ESR on protons and the more complex proton ENDOR technique have proved to be powerful tools for the elucidation of the unpaired spin density distribution in free radicals. Additional information about molecular dynamics can be obtained from the temperature dependence of HFS constants and from relaxation processes determining the ESR/ENDOR line widths and intensities (hindered rotation, electron transfer processes, counterion and solvent effects).¹ Moreover, ESR spectra also show hyperfine splittings from magnetic nuclei other than protons, thus yielding more detailed insight into the magnetic behavior of organic molecules containing heteroatoms. An illustrative example is ¹⁴N ESR in the field of spin labeling in biological systems.² Obviously the most interesting nonproton nucleus for the organic chemist is the ¹³C isotope. ¹³C magnetic resonance spectroscopy gives more direct structural information on the carbon skeleton than proton spectroscopy does, furthermore the spin density at carbon atoms without attached protons can only be extracted from the ¹³C couplings. Unfortunately, ESR on ¹³C in natural abundance (1.1%) often fails for intensity reasons and ¹³C enrichment is required for an unambiguous measurement of the ¹³C HFS constants from the ESR spectra. It has to be noted that the 2p_z-spin population on the carbon atom cannot be deduced from the ¹³C coupling constant using a McConnell type of formula. Its determination is somewhat more complicated because the spin populations at the adjacent carbon centers contribute to the spin density at the carbon nucleus under study and the Karplus-Fraenkel treatment has to be used.³

Obviously, ¹³C ENDOR in solution requires isotopically enriched samples. Previously, ¹³C ENDOR resonances have been detected from perdeuteriobenzophenone ketyl radical with 90% ¹³C at the carbonyl carbon.⁴ However, the signal-to-noise ratio of the respective ENDOR lines was rather poor, clearly indicating the experimental difficulties in the detection of the ¹³C resonances.

In the present communication we describe the reinvestigation of the feasibility of ¹³C ENDOR spectroscopy. For this purpose we have chosen the galvinoxyl system, which has proved to be very useful in studying dynamic effects in the doublet state molecules, such as hindered rotation,⁵ and the influence of the electron-electron exchange and dipolar interaction in the respective biradicals by using ESR and ¹H ENDOR.⁶ The ¹³C labeled galvinoxyl precursors can be obtained by an organolithium synthesis, which we have recently described.⁷

In order to perform successful ¹³C ENDOR experiments

we first have to look for the optimum ENDOR conditions, i.e. signal to noise ratio, resolution, and temperature region. By studying the temperature dependence of the ¹H and especially the ¹³C HFSC's we should be able to get an insight into the mechanism of dynamic processes, e.g. changes in hybridization of the central carbon.

From the biradical ENDOR study significant changes of the HFSC's are expected, as compared to the corresponding monoradical. The magnitude of these changes should be dependent on the molecular position of the magnetic nuclei, i.e., the phenyl ring protons and the central ¹³C nucleus. Furthermore, the different relaxation behavior of the monoradical and the respective biradical should show up in the ENDOR spectra.^{6c}

Theory

The appropriate spin Hamiltonian for a doublet radical is given by

$$\mathcal{H} = \beta B_0 g S - \sum_i \beta_N g_N B_0 I_i + h \sum_i S A_i I_i \quad (1)$$

including the electron and nuclear Zeeman and the hyperfine interaction terms. *A_i* represents the hyperfine coupling tensor (HFST) of nucleus *i* in frequency units. In fluid solution only the isotropic part *a_i* = 1/3 Tr(*A_i*) of the HFST is observed. When dealing with biradicals the spin Hamiltonian has to be expanded by the dipolar coupling and the scalar exchange interaction of the two electrons with $|J| \gg |a|$ yielding

$$\mathcal{H} = \beta B_0 g S - \sum_i \beta_N g_N B_0 I_i + h \sum_i S A_i I_i + D(S_z^2 - 1/3 S^2) + E(S_x^2 - S_y^2) + 1/2 J(S^2 - 3/2) \quad (2)$$

The hyperfine interaction is described by effective triplet coupling parameters *A_i*¹, which are directly given by the distances of the respective ESR HFS components. The isotropic HFSC of a biradical in solution *a_i*¹ (for definition see ref 17) can only be observed if the coupling is sufficiently large. Small HFSC's are usually obscured by the large line widths caused by the modulation of the zero-field splitting (EED).^{8,9}

More information may be obtained by using ENDOR with its much higher resolution. Applying the ENDOR selection rules $\Delta M_S = 0$, $\Delta M_I = \pm 1$ to the eigenvalues in the high-field approximation, derived from eq 1, the ENDOR resonance condition is given by

$$\nu_i^{\text{ENDOR}} = |\nu_N - M_S a_i| \quad (3)$$

where ν_N is the free nuclear frequency ($\nu_N = \beta_N g_N B_0 / h$) and $M_S = \pm 1/2$ for a doublet radical with isotropic HFSC a_i . Equation 3 remains valid for a biradical, provided that a_i is replaced by a_i' . Besides a pair of lines corresponding to $M_S = \pm 1$, an ENDOR line at the free nuclear frequency owing to $M_S = 0$ might be expected in biradicals but is found to be absent in isotropic solution.^{6c}

The theory of the ENDOR response was developed by Freed¹⁰ from Redfield's relaxation theory.¹¹ Freed's theory gives explicit solutions to the time-dependent density matrix as a function of the elements of the various magnetic interaction tensors and the correlation times of the respective modulation mechanisms (rotation, internal motion, etc.). A phenomenological description of the ENDOR experiment is given in ref 1b.

From the theory we might expect the following behavior of the ^{13}C nucleus in the ENDOR spectra as compared to protons:

(i) From the saturation condition for the nuclear transitions $\sigma_N = 1/4 \gamma_N^2 B_{\text{NMR}}^2 T_{2N} \Omega_N > 1$ it is obvious that the required saturating RF field B_{NMR} is much higher for carbon-13 than for protons, since $\gamma_{^{13}\text{C}}/\gamma_{\text{H}} \approx 1:4$ and usually the relaxation parameters $T_{2N} \Omega_N$ are smaller for ^{13}C . T_{2N} is the reciprocal ENDOR line width and Ω_N is Freed's saturation parameter for the nuclear transition observed.¹⁰

(ii) Since the ^{13}C HFS anisotropy usually is relatively large as compared to protons, modulation of the electron nuclear dipolar interaction (END) causes larger nuclear spin-lattice relaxation rates W_N for carbon-13. Therefore we expect an optimum ENDOR response ($W_N \approx W_e$) for this nucleus at shorter correlation times τ_C , i.e., higher temperatures and/or lower viscosities of the solution, since $W_N/W_e \propto \tau_C^2 \propto (\eta/T)^2$ is valid in the slow tumbling limit $\omega_e^2 \tau_C^2 \gg 1$.^{1b} The END mechanism also causes cross-relaxation effects $W_{X1,2}$, which might influence the ENDOR spectra at elevated temperatures.^{4,15}

(iii) ENDOR line widths are mainly determined by the electron spin-lattice relaxation rates W_e and additionally by nuclear relaxation. Thus, a larger line width is expected for carbon-13 as compared to protons.¹²

Experimental Section

Preparation of Compounds. All the ^{13}C labeled galvinols were obtained following our novel organometallic synthetic pathway described previously yielding mono and oligo galvinols.⁷ Corresponding to this procedure the diamagnetic precursors of the galvinoxyl radicals of the present work were prepared by treating the respective carboxylic esters or carbon dioxide with (2,6-di-*tert*-butyl-4-lithium phenoxy)trimethylsilane and by subsequent elimination of the protecting trimethylsilyl group. The ^{13}C labeled carboxylic esters were obtained by performing the known reaction of the organometallic components, derived from the appropriate halide, with $^{13}\text{CO}_2$, followed by esterification. The $^{13}\text{CO}_2$ is accessible from commercial $\text{Ba}^{13}\text{CO}_3$ (^{13}C content 90%).

It is noteworthy that the direct formation of **3a** from three molecules of the organolithium reagent and one molecule of $^{13}\text{CO}_2$ is unusual, clearly indicating the high reactivity of the organometallic compound. Actually, the convenient type of this reaction is known to give only the respective carboxylic acid.

Due to the high price of the $\text{Ba}^{13}\text{CO}_3$, all synthetic steps involving $^{13}\text{CO}_2$ were performed in an apparatus, allowing the $^{13}\text{CO}_2$ to escape from the parent $\text{Ba}^{13}\text{CO}_3$ and subsequent organometallic reaction under vacuum conditions.¹³

[(3,5-Di-*tert*-butyl-4-hydroxyphenyl)(3,5-di-*tert*-butyl-4-oxocyclohexa-2,5-dienylidene)methyl]benzene (1a). Bromobenzene (3.93 g), 0.61 g of Mg, and $^{13}\text{CO}_2$ from 3.95 g of $\text{Ba}^{13}\text{CO}_3$ yield 2 g of benzoic acid-(carboxyl- ^{13}C); 0.5 g of benzoic acid-(carboxyl- ^{13}C), 2.5 mL of thionyl chloride, and 15 mL of methanol yield 0.4 g of methyl ester; 0.4 g of benzoic acid methyl ester-(carbonyl- ^{13}C), 3.6 g of (2,6-di-*tert*-butyl-4-bromophenoxy)trimethylsilane, 6.3 mL of *n*-butyllithium in *n*-hexane (20%), and 1.8 mL of tetramethyldiami-

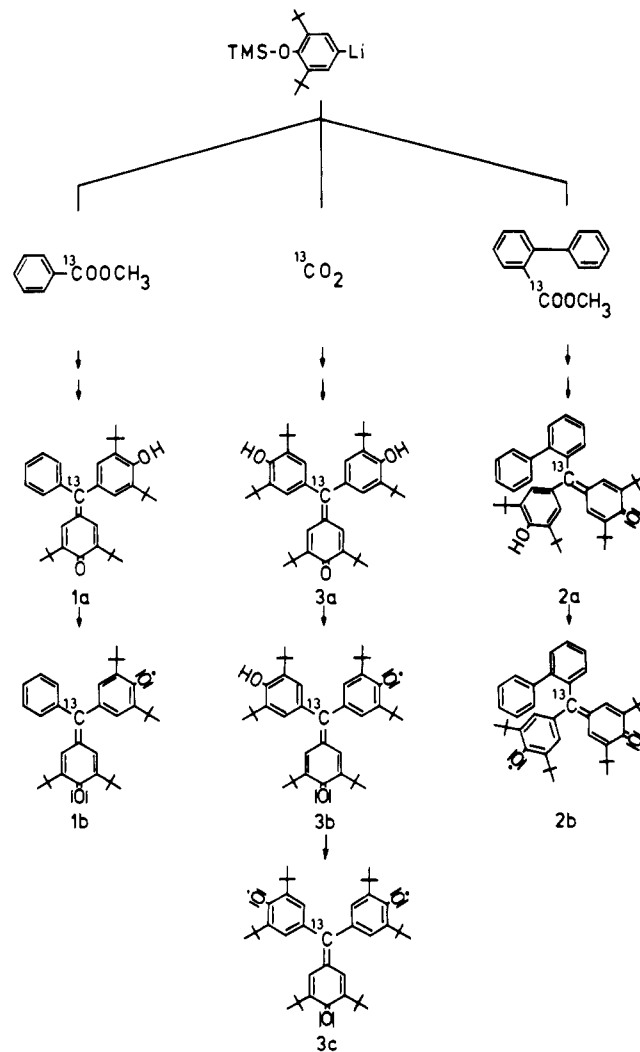


Figure 1. Reaction scheme for the preparation of the ^{13}C labeled galvinols and galvinoxyl radicals; note numbering of compounds.

noethane yield 0.5 g of **1a**.

2-[(3,5-Di-*tert*-butyl-4-hydroxyphenyl)(3,5-di-*tert*-butyl-4-oxocyclohexa-2,5-dienylidene)methyl]biphenyl (2a). 2-Iodobiphenyl (3.5 g), 0.31 g of Mg, and $^{13}\text{CO}_2$ from 1.98 g of $\text{Ba}^{13}\text{CO}_3$ yield 1.1 g of 2-biphenylcarboxylic acid-(carboxyl- ^{13}C); 0.4 g of 2-biphenylcarboxylic acid-(carboxyl- ^{13}C), 25 mL of thionyl chloride, and 20 mL of methanol yield 0.3 g of 2-biphenylcarboxylic acid methyl ester-(carbonyl- ^{13}C); 0.3 g of 2-biphenylcarboxylic acid methyl ester-(carbonyl- ^{13}C), 1.8 g of (2,6-di-*tert*-butyl-4-bromophenoxy)trimethylsilane, 3.3 mL of *n*-butyllithium in *n*-hexane (20%), and 0.9 mL of tetramethyldiaminoethane yield 0.6 g of **2a**.

Bis(3,5-di-*tert*-butyl-4-hydroxyphenyl)(3,5-di-*tert*-butyl-4-oxocyclohexa-2,5-dienylidene)methane (3a). (2,6-Di-*tert*-butyl-4-bromophenoxy)trimethylsilane (3.5 g), 6.1 mL of *n*-butyllithium in *n*-hexane (20%), 1.75 mL of tetramethyldiaminoethane, and $^{13}\text{CO}_2$ from 0.39 g of $\text{Ba}^{13}\text{CO}_3$ yield 0.4 g of **3a**.

The chemical properties of compounds **1a** to **3a** are identical with those given in ref 7.

The ^{13}C contents of the galvinols **1a-3a** were determined by mass spectroscopy (CH-5-D Varian MAT) at low voltages (<30 eV), where the ejection of hydrogen is no longer observed. The results were as follows: **1a** (91 \pm 3%); **2a** 91%; **3a** 89%.

The galvinoxyl radicals were prepared on a vacuum line following our procedure recently described,^{6b} i.e., treating carefully degassed toluene solutions of the galvinols with lead dioxide in the ESR/ENDOR sample tube, allowing distillation of the solvent under high vacuum conditions for concentrating, and diluting, respectively.

To generate the doublet radical **3b** from **3a** being free from the second oxidation step product, i.e., biradical **3c**, only part of the solution of **3a**, was oxidized and then mixed with another part of the

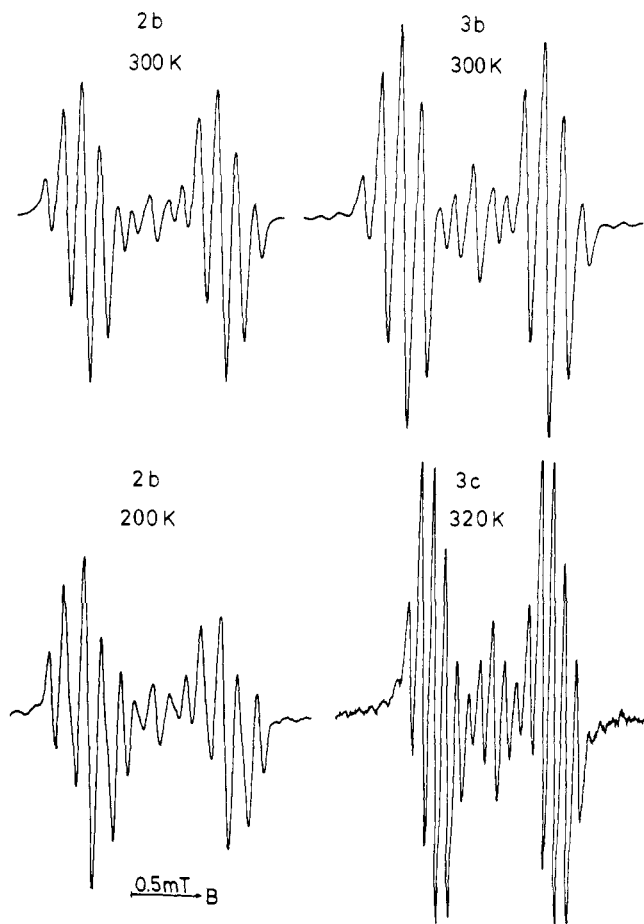


Figure 2. Solution ESR spectra of biphenylgalvinoxyl **2b** at 300 K and 200 K (left); comparison of the solution ESR spectrum of Yang's biradical **3c** at 320 K with the respective monoradical **3b** at 300 K (right).

solution of the parent compound **3a**. To complete the generation of **3c**, the galvinoxyl **3a** was allowed to react with lead dioxide until the doublet radical resonance was no longer observed in the ESR glass matrix spectrum, vide infra.

Instrumentation. To registrate the ESR spectra a commercial AEG 20-X spectrometer was used. ENDOR and TRIPLE spectra were recorded on a broad band spectrometer built in the Institut für Molekülphysik, Freie Universität Berlin, which has already been described,¹⁴ and on a commercial AEG ENDOR accessory, respectively (ENDOR spectra only). Temperature variation was achieved with an AEG temperature control unit; temperature data are accurate within ± 3 K.

Results

ESR. Monoradicals. Figure 2 pictures the pair of quintets HFS spectra of the monoradicals **1b**, **2b**, and **3b**. The weaker lines in the center of the spectra are due to the residual unlabeled compounds; their intensity amounts to about 10% of the overall absorption. The five-finger pattern with line intensities of 1:4:6:4:1 arising from the four equivalent ring protons of the galvinoxyl fragment is characteristic of an unlabeled aryl-substituted galvinoxyl system ($a = 3.7$ – 3.8 MHz). The larger doublet splitting ($a = 27.4$ – 27.7 MHz) clearly reveals the isotropic hyperfine coupling of the ^{13}C nucleus. The relatively large line widths are due to the unresolved HFS of the *tert*-butyl and phenyl ring protons. The intensities of the two quintets are nearly equal at room temperature, but on lowering the temperature the amplitudes of the high-field quintet become smaller and correspondingly broader than those of the low-field quintet. Moreover, in the low-temperature spectrum (200 K) of radical **2b** the five-lines pattern no longer exhibits the usual binomial intensity ratio. The second and the fourth

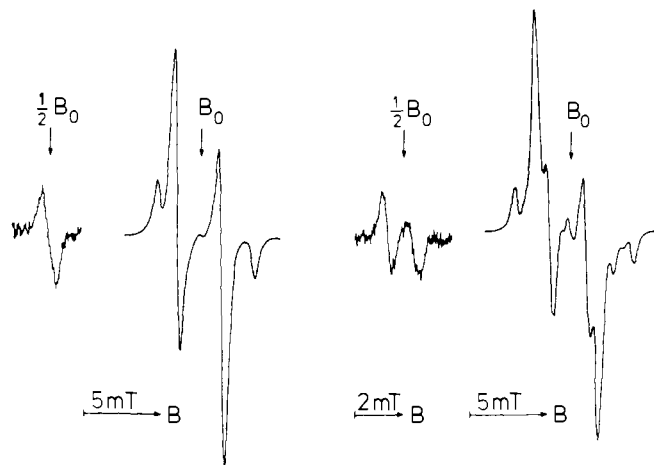


Figure 3. ESR glass spectra of Yang's biradical (left) and for the ^{13}C labeled Yang's biradical (right); additionally the respective half-field transitions are shown (toluene, 150 K).

lines are broader than the other ones and show a kink, indicating a forthcoming inequivalence of the galvinoxyl ring protons. The decrease of the ^{13}C HFSC of compound **2b** of 1% when cooling from 300 to 200 K is not substantially larger than in **1b** and **3b**.

Biradicals. The pair of septet hyperfine splittings of biradical **3c** (320 K) can readily be interpreted by assuming a coupling of six equivalent ring protons ($a^1 = 2.45$ MHz) and one ^{13}C nucleus ($a^1 = 24.2$ MHz), see Figure 2. On cooling, considerable line broadening occurs, indicating the increasing contribution of the anisotropic dipolar coupling of the unpaired electrons to the line width. The intensity difference between the low- and high-field groups is no longer observable in **3c**.

Figure 3 depicts the glass spectra of the labeled and unlabeled Yang's biradical **3c** obtained from a rigid matrix of supercooled toluene. The spectrum of the unlabeled compound shows two pairs of lines. Their spacing is determined by the ZFS parameter D , the distance between the xy and z components being D and $2D$, respectively ($D = 90$ MHz). The centers of gravity of the xy and z components do not coincide arising from the anisotropy of the g factor ($g_{\parallel} = 2.0031$, $g_{\perp} = 2.0056$). The glass spectrum of the isotopically enriched sample **3c** shows an additional splitting of the fine structure components due to hyperfine interaction with the ^{13}C nucleus. This splitting is most clearly perceptible in the high-field z component; the small peak in the middle of the pair of z lines arises from residual unlabeled compound. On the low-field side, only one z peak is resolved, the other line coincides with a xy peak. The splitting of the xy components (18.2 MHz) is about half as large as that of the z components (36.2 MHz).

The randomly oriented sample of Yang's biradical also exhibits a weak half-field transition, which is split into two lines when dealing with the ^{13}C labeled compound **3c**. The splitting is on the order of 27 MHz.

ENDOR. The upper spectra in Figures 4–6 show the high-resolution proton ENDOR spectra, taken at low temperatures, at weakly saturating RF fields and at microwave power $P_{\text{mw}} = 20$ mW and low amplitude of the 10 kHz FM of the RF field (20 kHz). The achieved unsaturated proton ENDOR line width was about 25 kHz, which enabled us to resolve even the smallest splittings, e.g., see insert in Figure 4 (amplitude of the 10 kHz FM of the RF field ± 5 kHz, RF power 1 G amplitude in the rotating frame). In these spectra the ^{13}C ENDOR lines do not show up. Taking account of the required ^{13}C ENDOR conditions the other ENDOR spectra have been recorded using higher temperatures and higher NMR power levels (see figure captions).

Table I. Proton and ^{13}C Hyperfine Coupling Constants^a

	<i>a</i> , MHz	1b ^b	2b ^b	3b ^b	3c ^c
Galvinoxyl moiety	^{13}C	-27.73	-27.27	-27.24	-24.15
	H _m	+3.57, +3.71	+2.84, +2.98, +4.13, +4.26	+3.60	+2.40
	H _{i-Bu}	+0.13	+0.13	+0.13	
Substituent	H _o	+0.56		+0.65	
	H _m	-0.20	0.37, 0.47		
	H _p	+0.62			

^a All HFSC's are measured by ENDOR, accurate within ± 0.01 MHz. ^b In **1b** to **3b** the H HFSC's are determined at 200 K, the ^{13}C HFSC's at 230 K. ^c In **3c** H and ^{13}C HFSC's are measured at 260 K.

Figure 4 shows ENDOR spectra from ^{13}C phenyl galvinoxyl **1b** in toluene at two different temperatures. The high-resolution spectrum (top) was taken at about 190 K; the insert depicts the obtained resolution in the center of the spectrum. All resonance lines are equally spaced around the free proton frequency at $\nu_{\text{H}} = 14.03$ MHz, as indicated in the figure. We deduced six proton HFSC's; the values are collected in Table I. Sign determination of all HFSC's was achieved by TRIPLE resonance¹⁴ with respect to the ring proton couplings of the galvinoxyl moiety which can safely be assumed to be positive.

Increasing the above-mentioned parameters as indicated we obtained the spectrum shown in the lower part of Figure 4. Now the ^{13}C ENDOR lines clearly show up, separated by $2\nu_{^{13}\text{C}} = 7.11$ MHz and equally spaced around $\frac{1}{2} a_{^{13}\text{C}} = 13.88$ MHz, which is very close to ν_{H} . This case is expected from eq 3, if $\nu_{\text{N}} < |a_i/2|$ is valid. At higher temperatures the ^{13}C ENDOR enhancement increases considerably (vide infra), but the resolution of the proton lines is decreased progressively.

In contrast to the proton lines, the ^{13}C transitions are considerably less saturated. The amplitudes of the ^{13}C ENDOR lines are significantly different, owing to the HFS enhancement factor. At 230 K the intensity of each ^{13}C ENDOR line remains unaltered when switching the external field from one ^{13}C m_I component to the other in ESR. Hence, at 230 K cross-relaxation effects are negligible. Even at room temperature, the quotient of the ENDOR amplitudes when saturating the low and high field ESR transition, respectively, is much less than 2. However, at higher temperatures W_{X2} processes dominate the ^{13}C ENDOR spectra of all galvinoxyls studied. A more detailed investigation of the relaxation behavior of the ^{13}C nucleus is found elsewhere.¹⁵

In Figure 5 ENDOR spectra of 2-biphenylgalvinoxyl (**2b**) are presented. From the high-resolution spectrum at 200 K (top) we deduced seven proton HFSC's (Table I). The center of the spectrum could not be resolved further. These small HFSC's can be assigned to the biphenyl and *tert*-butyl protons. It is noticeable that in radical **2b** all four galvinoxyl ring protons are inequivalent at this low temperature, while in **1b** there are only two sets of HFSC's for these positions. Although spectral resolution is diminished at elevated temperatures, dynamic effects clearly show up, resulting in only one averaged HFSC for all galvinoxyl ring protons. The lower part of Figure 5 pictures the ENDOR spectrum of **2b** at higher temperature (for experimental conditions see figure caption). The ^{13}C couplings are similar in radicals **1b** and **2b** (see Table I). In good agreement with the ESR results the ENDOR spectra do not show a marked change in the ^{13}C HFSC with temperature.

Figure 6 demonstrates the increase of ^{13}C ENDOR amplitudes with increasing temperature using monoradical **3b** as a model compound. At high-resolution conditions (180 K) **3b** shows three pairs of proton ENDOR lines. In the spectra taken at 200 K and at higher temperatures additionally the ^{13}C ENDOR lines show up.

In Figure 7 the ENDOR spectra of ^{13}C Yang's biradical **3c**



Figure 4. ENDOR spectra taken from ^{13}C phenylgalvinoxyl **1b** at different experimental conditions; (top) 190 K, $B_{\text{NMR}} = 2G_{\text{rot}}$, for insert see text; (bottom) 230 K, $B_{\text{NMR}} = 6.2G_{\text{rot}}$.

(solid line) and of the corresponding monoradical **3b** (broken line) are compared. In the biradical spectrum the ENDOR resonance condition is $\nu_{\text{ENDOR}} = |\nu_{\text{N}} \pm a^t|$. We deduced the ring proton and the ^{13}C HFSC's given in Table I. The resonance line at the free proton frequency could not be resolved further. Since the presence of monoradical impurities could be excluded and since recent considerations have shown that the "free proton frequency line" ($M_S = 0$) of a biradical should not show up in the solution ENDOR spectrum, we assigned this line to the *tert*-butyl protons of the biradical. The ^{13}C ENDOR resonances in biradical **3c** are equally spaced around $a_{^{13}\text{C}}$ owing to the modified ENDOR resonance condition for a triplet spin state (see eq 3). Thus the ^{13}C ENDOR lines are shifted significantly to higher frequencies in the spectrum of **3c**, see Figure 7. The proton HFSC's show up around the free



Figure 5. ENDOR spectra taken from ^{13}C biphenyl galvinoxyl **2b** at different experimental conditions: (top) 200 K, $B_{\text{NMR}} = 2.7G_{\text{rot}}$, (bottom) 220 K, $B_{\text{NMR}} = 6.2G_{\text{rot}}$.

proton frequency in both spin states (**3b** and **3c**), being quite different in magnitude, see Table I. As expected the HFSC of the ring protons in the biradical is about $2/3$ of the respective coupling in the monoradical.

Discussion

Signs and Assignments of HFSC's. As can be seen from Table I, signs and magnitudes of all possible proton HFSC's could be determined for the phenylgalvinoxyl radical **1b**. Assignments to molecular positions were achieved by comparison with other galvinoxyl systems. The conventional sequence $|a_p| > |a_o| > |a_m|$ in the phenyl substituent seems to be reasonable, since the twist angle was estimated to be much smaller than 65° , therefore excluding large effects from phenyl hyperconjugation.¹⁶ At first sight it is surprising that the signs of HFSC's in the phenyl ring are reversed as compared to what is usually found, that is $a_o, a_p < 0, a_m > 0$. This sign reversal obviously indicates that the phenyl ring is attached to a carbon with negative $2p_z$ spin density. These findings can be understood, since the molecular orbital occupied by the unpaired electron has a node at the central carbon atom, spin density therefore arising only from π - π spin polarization. This was confirmed by a very recent McLachlan calculation.¹⁸ Consequently, the calculations also give the correct signs of carbon π spin densities in the phenyl ring, yielding the reversed signs of all proton HFSC's.

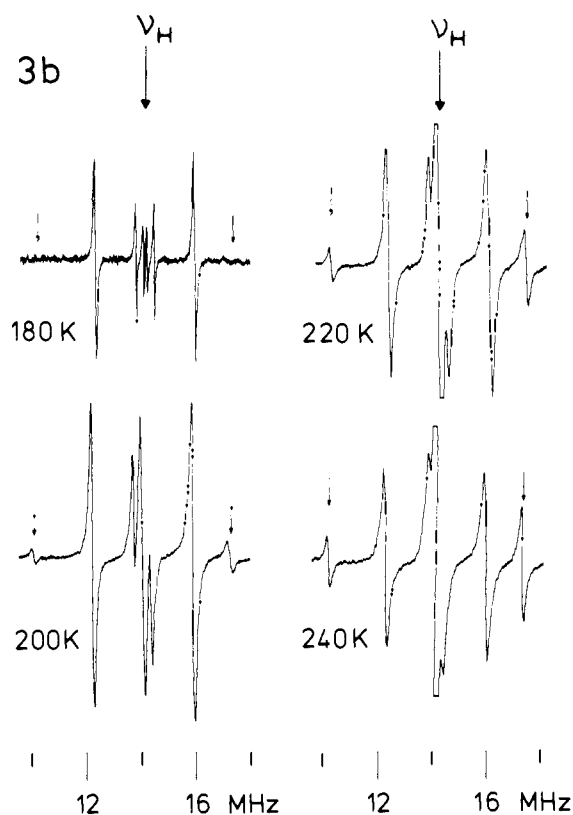


Figure 6. ENDOR spectra obtained from radical **3b** at four different temperatures. The spectrum at 180 K is taken at $B_{\text{NMR}} = 4.3G_{\text{rot}}$, the other spectra at $B_{\text{NMR}} = 6.2G_{\text{rot}}$. The arrows on both sides of the spectra indicate the positions of ^{13}C ENDOR lines.

The sign of the ^{13}C HFSC was derived from the observed m_1 -dependent line width variation in the ESR spectrum (Figure 2), described by $T_2^{-1}(m_1) = A + Bm_1 + Cm_1^2$. Provided the sign of B in this equation is known, the sign of the HFSC from the nucleus responsible for the observed line width effect becomes accessible. B is proportional to the inner product of the anisotropic g and A tensor ($g':A'$) which equals $3/2 A'_{zz}g'_{zz}$ for a molecule with cylindrical symmetry. In approximately planar π radicals g'_{zz} is generally negative,¹⁷ and the sign of A'_{zz} is determined by the $2p_z$ -spin population at the ^{13}C nucleus in the galvinoxyl radicals, which was calculated to be negative. Thus, B should be positive, resulting in a broadening of the $m_1 = 1/2$ ESR component. Experimentally we find the high-field ESR line to be broadened, indicating a negative sign of the isotropic ^{13}C HFSC, since the resonance fields are given by $B_{\text{res}}(m_1) = B_0 - am_1$. All the above given signs of the HFSC's were confirmed by our TRIPLE resonance experiments (Table I).

Using the Karplus-Fraenkel relation³ and the calculated $C 2p_z$ spin populations from ref 18, a ^{13}C HFSC of -17.4 MHz was obtained. The deviation from the experimental value (-27.73 MHz) is probably an effect of the angular dependence of the Q -parameters in the Karplus-Fraenkel treatment or may be due to an inaccuracy of the McLachlan data used.

The spin density distribution in the other galvinoxyls **2b** and **3b** is expected to be very similar to **1b**, being consistent with our experimental results (Table I).

The reduced proton HFSC in Yang's biradical **3c**, as compared to the corresponding monoradical **3b** ($a^1 \approx 2/3 a^d$) clearly indicates $|J| \gg |a|$, i.e., the unpaired electrons are delocalized over the whole π system. The ^{13}C HFSC is only reduced by about 10%, because the probability of finding an unpaired electron at the central carbon should remain unaltered in the doublet and in the respective triplet spin system. The small

deviation of $a^d_{13\text{C}}$ from $a^i_{13\text{C}}$ can readily be understood, assuming small changes in the electronic structure and conformation, caused by the hydroxyphenyl substituent in monoradical **3b**.

Dynamic Effects. Very recently dynamic effects have been observed in the ESR/ENDOR spectra of some substituted galvinoxyl radicals.⁵ As described above, the galvinoxyl ring proton HFSC's are strongly influenced by temperature changes. However, the ^{13}C HFSC is not altered very much (3–5 kHz/K in **1b** to **3b**). Since ^{13}C HFSC's are known to be very sensitive to changes in molecular structure,³ and even to changes in the molecular environment,¹⁹ we conclude the electronic and structural surroundings of the central carbon to remain nearly unaffected. Therefore, the dynamic effects observed in the proton spectra cannot be explained by a "pyramidal atomic inversion", involving changes in hybridization, but by hindered rotation, i.e., a jump process, which does not influence the equilibrium conformations of the galvinoxyl radical.

In **1b** two slightly different galvinoxyl ring proton HFSC's are deduced at lower temperatures, which can be assigned to the "inner" and "outer" protons in the equally twisted galvinoxyl rings. In **2b** the C_2 symmetry is lifted, resulting in an inequivalence of the galvinoxyl rings caused by different twist angles. Thus we find four inequivalent meta protons. It is noteworthy that the averaged proton HFSC's in all four positions (3.55 MHz) do not significantly deviate from those in **1b** (3.64 MHz) and **3b** (3.60 MHz). At elevated temperatures all the HFSC's from the galvinoxyl ring protons in **1b** and **2b** become equivalent by the dynamic process, and only the averaged couplings are observed.

Glass Spectra. The glass spectrum of the ^{13}C labeled biradical is of considerable interest, because the fine structure components are additionally split by the ^{13}C hyperfine interaction. Therefore the principal values of the complete HFS tensor could be extracted. Since the x and y components in Yang's biradical coincide ($E \approx 0$), axial symmetry can safely be assumed. Thus, the principal axes of the zero-field splitting tensor (ZFST) and the hyperfine tensor (HFST) are identical. Hence, the splittings of the ZFS components directly give the principal values of the HFST (150 K):

$$a^i = (-24.20 \pm 0.1) \text{ MHz}$$

$$A'_{xx} = A'_{yy} = (+6.0 \pm 0.2) \text{ MHz}$$

$$A'_{zz} = (-12.0 \pm 0.2) \text{ MHz}$$

The alternative with all signs reversed can be ruled out for the following reasons:

(i) In analogy to the calculated negative C $2p_z$ spin density¹⁸ for the central carbon in phenylgalvinoxyl **1b**, the A'_{zz} component in the biradical, exhibiting similar geometry, should also be negative; (ii) the negative sign of the isotropic ^{13}C HFSC could be confirmed by TRIPLE resonance in solution (vide supra).

The unsymmetric line shape of the split half-field transition (Figure 3) may be accounted for by analogy to the powder spectrum of a monoradical. The observed spectrum is a superposition of the spectra for all molecular orientations; the line positions depend on the anisotropic values of the g factor and the ^{13}C HFSC. Shifts from the ZFS may be neglected due to the small D value (90 MHz). The isotropic ^{13}C HFSC cannot be obtained directly from this spectrum because the anisotropies are not negligibly small. However, the splitting is of the same order of magnitude as in the high-field region.

Comparison of ^{13}C and ^1H Nuclear Relaxation. From Figure 6 it becomes obvious that optimum proton and ^{13}C ENDOR signal intensities call for modified experimental conditions, e.g.,

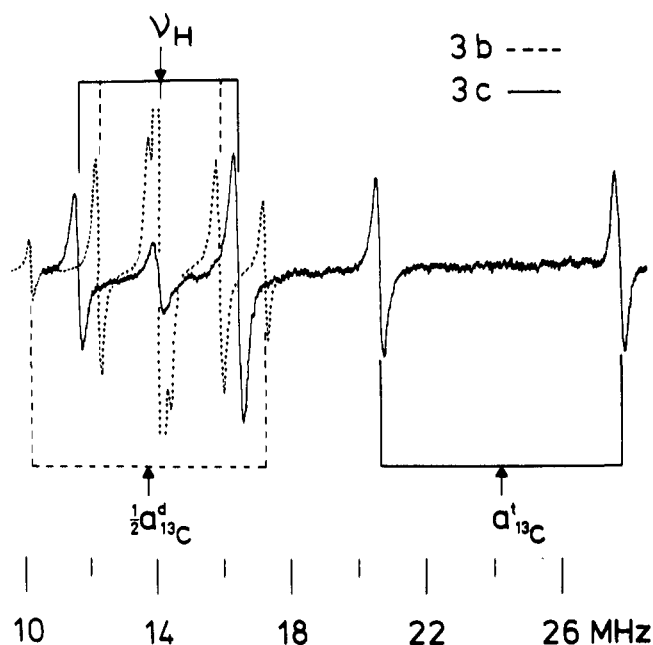


Figure 7. Comparison between the ENDOR spectra of ^{13}C Yang's biradical **3c** (solid line, 260K, $P_{\text{mw}} = 100 \text{ mW}$, $B_{\text{NMR}} = 6.2G_{\text{rot}}$) and the respective monoradical **3b** (broken line, 240 K, $P_{\text{mw}} = 20 \text{ mW}$, $B_{\text{NMR}} = 6.2G_{\text{rot}}$). In the biradical the ^{13}C ENDOR lines were taken at the same induced nuclear transition rates.

temperature and RF power. Since both nuclei have no quadrupole moments ($I = 1/2$), nuclear relaxation is mainly determined by the END interaction depending on the magnitude of the anisotropic HFS, i.e., $\text{Tr}(A'^2)$. For protons and carbon-13 $\text{Tr}(A'^2)$ usually is in the order of 1–100 MHz^2 and 10–1000 MHz^2 , respectively. To gain a better insight into nuclear relaxation present in the radicals under study, we have performed saturation measurements on a proton ENDOR line (15.73 MHz) and on a ^{13}C ENDOR line (17.15 MHz) of **3b** at 240 K. The unsaturated line widths are about 70 kHz for protons and 100 kHz for carbon-13. The ratio of the measured nuclear spin-lattice relaxation rates $\Omega_{\text{H}}:\Omega_{\text{C}} \approx W_{\text{C}}:W_{\text{H}}$ equals 32 ± 5 . Since both nuclei are part of the same molecule, the ratio of the nuclear relaxation rates should be equal to that of the different HFS anisotropies $\text{Tr}(A'^2)$.^{1b,10}

McConnell and Strathdee²⁰ have calculated the principal values of the anisotropic HFST in a C–H fragment, using unit spin density in the carbon $2p_z$ orbital: $A'_{xx}(\text{H}) = +43.33$, $A'_{yy}(\text{H}) = -38.66$, and $A'_{zz}(\text{H}) = -4.66$ MHz. Assuming axial symmetry and unit C $2p_z$ spin density for a central carbon atom one obtains $A'_{zz}(\text{C}) = +181.6$, $A'_{xx}(\text{C}) = A'_{yy}(\text{C}) = -90.8$ MHz.¹⁷ Based on the calculated McLachlan π spin densities in phenylgalvinoxyl [$\rho(\text{C}_{\text{central}}) \approx -0.062$],¹⁸ the principal values of the anisotropic HFST for the central carbon-13 are as follows: $A'_{zz}(\text{C}) = -11.3$, $A'_{xx}(\text{C}) = A'_{yy}(\text{C}) = +5.65$ MHz. It is remarkable that these data are in good agreement with our experimental results for the ^{13}C HFST in the biradical **3c**.

Using the calculated [$\rho(\text{C}_{\text{meta}}) = -0.043$]¹⁸ and neglecting contributions from neighboring carbon atoms, the principal values of the HFST for the respective galvinoxyl meta proton are: $A'_{xx}(\text{H}) = -1.86$, $A'_{yy}(\text{H}) = +1.66$, $A'_{zz}(\text{H}) = +0.20$ MHz. Thus, $\text{Tr}(A'^2)$ equals 6.25 MHz^2 for the meta protons and 192.0 MHz^2 for the central carbon-13, yielding a quotient of 30.7. This estimation on the basis of calculated data is in good agreement with the quotient of the experimentally determined nuclear relaxation rates.

ENDOR Line Width and Saturation Behavior. In positions of high π spin densities, e.g., at the central carbon in triphen-

ylmethyl radicals, $\text{Tr}(A'C^2)$ exceeds values of 1000 MHz², resulting in significantly enlarged nuclear relaxation rates. Thus the ¹³C ENDOR lines are broadened and saturation becomes more difficult, due to a faster spin-lattice relaxation and increasing nuclear contributions to the line width. Recently, this fact has been experimentally verified on some labeled ketyl, aromatic hydrocarbon, and triphenylmethyl radicals, where the ¹³C transitions often could not be saturated with RF field amplitudes up to 30G_{rot} (275 K).¹⁵ However, in our radicals the anisotropy of the ¹³C nucleus is not very large, e.g., in **3b** the ¹³C transitions are already saturated at about $(11 \pm 2)G_{\text{rot}}$; RF saturation of the proton transitions was achieved at about $(5 \pm 1)G_{\text{rot}}$ (240 K, $P_{\text{mw}} = 20$ mW).

The applied RF fields B'_{NMR} required to saturate the ¹³C and proton transitions, respectively, can be estimated, taking account of the HFS enhancement factor $\nu_{\text{ENDOR}}/\nu_{\text{N}}$.¹⁷

$$B'_{\text{NMR}}(\text{C}) = \frac{\nu_{\text{H}}^{\text{ENDOR}} \nu_{\text{C}} \gamma_{\text{H}}}{\nu_{\text{H}} \nu_{\text{C}}^{\text{ENDOR}} \gamma_{\text{C}}} \left(\frac{T_{2\text{H}} \Omega_{\text{H}}}{T_{2\text{C}} \Omega_{\text{C}}} \right)^{1/2} \cdot B'_{\text{NMR}}(\text{H})$$

Using an enhancement factor of 4.8 for carbon-13 and of 1 for protons, equal values for $T_{2\text{N}}$, and the experimentally determined ratio of the nuclear relaxation rates $\Omega_{\text{H}}/\Omega_{\text{C}} \approx W_{\text{C}}/W_{\text{H}} = 32$, the saturating RF field for carbon-13 is expected to be about four times larger than that for protons, being in fair agreement with the experimental value of about 2, considering experimental errors and the simplifications, made in our estimation.

ENDOR Response. The optimum ENDOR response occurred at (200 ± 10) K for the galvinoxyl ring protons and at (260 ± 10) K for carbon-13, corresponding to the temperatures where W_{e} should equal W_{N} . Obviously, at room temperature for both kinds of nuclei $W_{\text{N}} < W_{\text{e}}$ is valid, requiring lower temperatures in order to increase the rotational correlation time τ_{C} , which is given by the Stokes-Einstein relation^{1b} to be $\tau_{\text{C}} \propto (\eta/T)$. From the measured temperatures and the viscosity data for toluene we can evaluate $[\tau_{\text{C}}(200 \text{ K})/\tau_{\text{C}}(260 \text{ K})]^2$ to be about 41 ± 10 . It can be shown²³ that this value should roughly reflect the value of $\text{Tr}(A'C^2)/\text{Tr}(A'H^2)$. This is in good agreement with experiment, vide supra.

In the foregoing considerations cross-relaxation effects have been neglected, being justified by our measurements. These effects are also caused by the END term ($\text{Tr}(A'^2)$) and exhibit a similar τ_{C} dependence as W_{e} , i.e., $W_{\text{X}}^{\text{END}} \propto 1/\tau_{\text{C}} \propto T/\eta$. Thus, for the galvinoxyl radicals studied, the magnitude of the ¹³C anisotropy does not allow large cross-relaxation effects to occur below 290 K. At higher temperatures a dominant $W_{\text{X}2}$ process (as compared to $W_{\text{X}1}$) shows up.

ENDOR on Biradicals. Optimum proton and ¹³C ENDOR lines of biradical **3c** in solution should be obtained at somewhat lower temperatures as compared to the respective monoradical, because the modulation of the electron-electron dipolar interaction (EED) causes an additional W_{e} process. Since the ENDOR enhancement is defined as the relative change of ESR amplitude and the latter is decreased drastically at low temperatures in biradicals, maximum proton ENDOR signals from **3c** are obtained at higher temperatures than from monoradical **3b** (cf. ref 6c). As is obvious from Figure 7 in the biradical at 260 K the ¹³C ENDOR lines could readily be observed being equal in intensity to the proton lines.

The larger ENDOR line widths in the biradical can easily be explained by the increased W_{e} , resulting in enhanced saturating mw fields required.

In the ENDOR spectra of **3c** in glassy solution (toluene, 150 K) the resonance absorptions at the free nuclear frequencies (ν_{H} and ν_{C}) could be observed with significantly diminished line widths (about 30 kHz), as compared to the solution spectra. The occurrence of these lines, due to nuclear spin transitions in the $M_{\text{S}} = 0$ manifold, can be understood, because

the EED interaction is not averaged out in frozen solution. Therefore, the two electron spin transitions ($| -1 \rangle \leftrightarrow | 0 \rangle; | 0 \rangle \leftrightarrow | +1 \rangle$) are no longer degenerate, permitting a selective pumping of either transition. Resonances from protons or carbon-13 exhibiting HFS are expected to be much lower in intensity; a more detailed discussion will be given elsewhere.²¹

It is quite interesting that the free ¹³C ENDOR line does not occur at position ν_{C} , calculated from the experimental ν_{H} , but is shifted by (114 ± 1) kHz to higher frequencies, measured on the *xy* as well as on the *z* components in the ESR glass spectrum. Assuming axial symmetry, the principal axes of the ZFST and HFST to be identical, and the electronic and nuclear *g* factors to be isotropic, we calculated the second-order contributions to the spin states belonging to $M_{\text{S}} = 0$. The second-order shift of the ENDOR transitions at the free nuclear frequency in a biradical amounts to

$$\delta\nu = A^2/\nu_{\text{e}}$$

In glassy matrix a fluctuation term can be neglected. Using the above given principal values of **3c**, the limiting second-order shifts amount to about 40 and 150 kHz, respectively. This evaluation confirms our assumption that the frequency shift observed can be explained by a second-order effect from the hyperfine interaction. The respective second-order shifts for ν_{C} of the monoradicals **1b**, **2b**, and **3b** in solution are in the order of 20–30 kHz and can easily be interpreted using $\delta\nu = \langle a^2 \rangle / 4\nu_{\text{e}}$, which depends upon the squared value of the isotropic HFSC a^2 and its mean square fluctuation caused by molecular motion.^{1b}

Conclusions

Concluding we can state that ¹³C ENDOR in liquid solution can easily be obtained from substituted galvinoxyl radicals and even from Yang's biradical. From the experimental results it is obvious that the optimum ¹³C ENDOR conditions as compared to those of protons are governed by the relative magnitudes of the HFS anisotropies: (i) In cases of large contributions from the ¹³C END interaction, maximum ¹³C ENDOR signals are obtained at elevated temperatures and strong cross-relaxation effects are observed.¹⁵ (ii) For very small ¹³C anisotropies, the carbon-13 nucleus behaves similar to protons.²² (iii) In the radicals studied, $\text{Tr}(A'C^2)$ is in between the limiting cases (i) and (ii), calling for somewhat higher temperatures and RF field amplitudes; however, cross-relaxation effects are negligible up to room temperature.

The investigation of ¹³C labeled organic compounds by magnetic resonance techniques has proved to be suitable in the elucidation of electronic structure and in unraveling complex dynamic processes. On the other hand, preparation of isotopically enriched compounds is highly expensive and time consuming. Thus we feel that the ENDOR studies presented in this paper may serve well as a prerequisite of more sophisticated natural-abundance ¹³C multiple resonance experiments on free radicals.

Furthermore, the observation of ENDOR lines at the free nuclear frequencies in biradicals opens an interesting aspect: In biradicals containing nuclei with $I \geq 1$, the elucidation of the quadrupole couplings of these nuclei should be possible. Experiments on this subject are in progress.

Acknowledgments. The authors wish to thank Dr. R. Biehl, H. J. Fey, Professor Dr. K. Möbius, and Dr. M. Plato, from Institut für Molekülphysik, Freie Universität Berlin, for many helpful discussions. Moreover we are indebted to Dr. M. Plato for helpful criticism of the manuscript and for his suggestions. We are grateful to the Institut für Molekülphysik for the use of their facilities. This work was supported by the Deutsche Forschungsgemeinschaft (DFG-Normalverfahren), which is

gratefully acknowledged. H. Kurreck is grateful to the Fonds der Chemischen Industrie for financial support.

References and Notes

- (1) (a) K. Scheffler and H. B. Stegmann, "Elektronenspinresonanz", Springer-Verlag, Berlin, 1970; (b) L. Kevan and L. D. Klisport, "Electron Spin Double Resonance Spectroscopy", Wiley, New York, N.Y., 1976, and references cited therein.
- (2) L. J. Berliner, Ed., "Spin Labeling", Academic Press, New York, N.Y., 1976.
- (3) M. Karplus and G. K. Fraenkel, *J. Chem. Phys.*, **35**, 1312 (1961).
- (4) K. P. Dinse, K. Möbius, R. Biehl, and M. Plato, *Magn. Reson. Relat. Phenom., Proc. Congr. AMPERE, 17th*, 419 (1973).
- (5) K. Hinrichs, B. Kirste, H. Kurreck, and J. Reusch, *Tetrahedron*, **33**, 151 (1977).
- (6) (a) W. Broser, B. Kirste, H. Kurreck, J. Reusch, and M. Plato, *Z. Naturforsch., B*, **31**, 974 (1976); (b) W. Gierke, W. Harrer, B. Kirste, H. Kurreck, and J. Reusch, *ibid.*, **31**, 965 (1976); (c) H. van Willigen, M. Plato, K. Möbius, K. P. Dinse, H. Kurreck, and J. Reusch, *Mol. Phys.*, **30**, 1359 (1975).
- (7) W. Harrer, H. Kurreck, J. Reusch, and W. Gierke, *Tetrahedron*, **31**, 625 (1975).
- (8) E. Wasserman, L. C. Snyder, and W. A. Yager, *J. Chem. Phys.*, **41**, 1763 (1964).
- (9) R. M. Dupeyre, H. Lemaire, and A. Rassat, *J. Am. Chem. Soc.*, **87**, 3771 (1965); R. Brière, R. M. Dupeyre, H. Lemaire, C. Morat, A. Rassat, and P. Rey, *Bull. Soc. Chim. Fr.*, 3290 (1965).
- (10) (a) J. H. Freed, *J. Chem. Phys.*, **43**, 2312 (1965); (b) *J. Phys. Chem.*, **71**, 38 (1967); (c) J. H. Freed, D. S. Leniart, and J. S. Hyde, *J. Chem. Phys.*, **47**, 2762 (1967); (d) J. H. Freed, *ibid.*, **50**, 2271 (1969); (e) J. H. Freed, D. S. Leniart, and H. D. Connor, *ibid.*, **58**, 3089 (1973).
- (11) A. G. Redfield, *Adv. Magn. Reson.*, **1**, 1 (1965).
- (12) W. Lubitz, K. P. Dinse, K. Möbius, and R. Biehl, *Chem. Phys.*, **8**, 371 (1975).
- (13) H. R. Schütte, "Radioaktive Isotope in der Organischen Chemie und Biochemie", Verlag Chemie, Weinheim, 1966; K. Schubert, Diplomarbeit, Freie Universität Berlin, 1976.
- (14) R. Biehl, M. Plato, and K. Möbius, *J. Chem. Phys.*, **63**, 3515 (1975).
- (15) H. J. Fey, Diplomarbeit, Freie Universität Berlin, 1977; to be published.
- (16) R. Biehl, K. Hinrichs, H. Kurreck, W. Lubitz, U. Mennenga, and K. Roth, *J. Am. Chem. Soc.*, **99**, 4278 (1977).
- (17) N. M. Atherton, "Electron Spin Resonance", Ellis Horwood, Chichester, 1973.
- (18) K. Mukai, T. Kamata, T. Tamaki, and K. Ishizu, *Bull. Chem. Soc. Jpn.*, **49**, 3376 (1976).
- (19) N. Hirota in "Radical Ions", E. T. Kaiser and L. Kevan, Ed., Interscience, New York, N.Y., 1968; J. H. Sharp and M. C. R. Symons in "Ions and Ion Pairs in Organic Reactions", M. Szwarc, Ed., Vol. 1, Wiley, New York, N.Y., 1972.
- (20) N. M. McConnell and J. Strathdee, *Mol. Phys.*, **2**, 129 (1959).
- (21) B. Kirste, H. Kurreck, K. Möbius, M. Plato, and H. van Willigen, to be published.
- (22) This case was realized in a very recent ENDOR study using a ^{13}C labeled phenoxyl type radical, to be published.
- (23) W. Lubitz, thesis, Freie Universität Berlin, Germany, 1977.

Ion Binding Studied Using Quadrupole Splittings of $^{23}\text{Na}^+$ Ions in Lyotropic Liquid Crystals. The Dependence on Surfactant Type

G. Lindblom,* B. Lindman,* and G. J. T. Tiddy*

Contribution from Physical Chemistry 2, Chemical Center, P.O.B. 740, S-220 07 Lund, Sweden, and Unilever Research, Port Sunlight Laboratory, Port Sunlight, Wirral, Merseyside L62 4XN, England. Received August 26, 1977

Abstract: Sodium-23 NMR quadrupole splittings (Δ) are reported for sodium ions in lyotropic liquid crystals prepared from a range of surfactants. The results are consistent with the hypothesis that the splittings are caused by distortion of the sodium ion hydration due to a thin layer of bound water at the lipid/water interface. Nonionic surfactants show no binding of sodium ions at the surface. For the anionic surfactants sodium octyl sulfate and sodium octyl sulfonate, the Δ values are consistent with diffuse layer binding. It is necessary to postulate a specific binding to describe the binding in sodium octanoate systems. The behavior of splittings at high water content in systems anionic surfactant-decanol-water indicates that there is no first-order phase transition between B and D lamellar phases. Instead, the B phase seems to be a continuation of the D phase.

Introduction

The lipid bilayer is an essential component of biological membranes. To understand membrane properties, and in particular the role of counterions, it is necessary to investigate the binding of ions to bilayers. The lamellar phase, which is formed in simple amphiphile-water mixtures, is an excellent model system for this purpose. In addition, sodium NMR is a good technique to investigate interactions between ions and surfactant head groups because of the observation of quadrupole splittings in these systems.¹ To date, studies of these systems have dealt mainly with spectroscopic problems, and have given little detailed information on the nature of the binding between counterions and head groups. In this paper we report the changes in ^{23}Na quadrupole splittings caused by surfactant concentration and chemical structure. The results enable more information to be obtained on the mechanisms responsible for the splittings, and also give some insight into counterion binding in different systems.

We have investigated the magnitudes of splittings in lamellar phases formed from both charged and uncharged lipids. The phase diagrams of the systems chosen have been mostly studied

previously by Ekwall et al.,² and in general the liquid crystal structures are well established. However, our results suggest that the "B" lamellar phase reported for several of the systems studied is not a separate phase from the normal D lamellar phase, and should not be represented by a separate area on the phase diagram.

Experimental Section

Most chemicals used were commercially available, and were used without further purification. Sodium di(2-ethylhexyl)sulfosuccinate (Aerosol OT, Fluka) was purified according to Park et al.³ Samples were usually prepared by mixing a weighed amount of the components in sealed tubes at elevated temperatures. For alkyl sulfates this can cause degradation, and in these cases mixing was achieved by agitation/centrifugation at room temperature. Phase homogeneity was checked by deuterium NMR for samples containing D_2O , and by x-ray diffraction for a number of other samples. NMR measurements were made as described previously,^{4,5} using wide line and pulsed NMR spectrometers. Large splittings (>15 kHz) were measured on the wide-line spectrometer (15.82 MHz) and small splittings on the pulsed spectrometer (23.81 MHz). The latter was used in conjunction with a Varian C-1024 CAT. Generally, the measurements are accurate